

Reactivity Studies of Mononuclear and Dinuclear Vanadium–Sulfide–Thiolate Compounds

Shawn C. Sendlinger,[†] John R. Nicholson,[†] Emil B. Lobkovsky,[†] John C. Huffman,[†] Dieter Rehder,[‡] and George Christou^{*†}

Department of Chemistry and Molecular Structure Center, Indiana University, Bloomington, Indiana 47405, and Institute of Inorganic and Applied Chemistry, University of Hamburg, D-2000 Hamburg 13, Germany

Received July 30, 1992

The synthesis, structure, and properties of $(\text{Me}_3\text{NBz})_2[\text{V}(\text{S}_2)_2(\text{SPh})]$ (**1**) and $(\text{Me}_3\text{NBz})_4[\text{V}_2(\text{S}_2)_2(\text{CS}_2)_4]$ (**2**) are described. Compound **1** is produced via oxidation of V(III) by elemental sulfur in a reaction mixture comprising VCl_3 , LiSPh , S , and NEt_4Cl in a molar ratio of 1:7:3:2. Compound **1** reacts with excess CS_2 to produce compound **2** in ca. 65% yield. Compound **1** crystallizes in monoclinic space group $P2_1/n$ with the following unit cell dimensions at -158°C : $a = 18.178$ (8) Å, $b = 8.843$ (2) Å, $c = 18.852$ (7) Å, $\beta = 107.06$ (2)°, and $Z = 4$. A total of 2807 unique reflections with $F > 3.00\sigma(F)$ were employed, and the structure solution was refined to conventional indices R and R_w of 5.65 and 5.63, respectively. The vanadium(V) center is ligated by three types of sulfur atoms, viz. one PhS^- , one persulfido (S_2^{2-}), and two sulfido (S^{2-}); the coordination geometry is approximately tetrahedral, with the S_2^{2-} considered as occupying one site. Compound **2** crystallizes in monoclinic space group $P2_1/c$ with the following unit cell dimensions at -114°C : $a = 20.978$ (4) Å, $b = 13.384$ (2) Å, $c = 21.613$ (4) Å, $\beta = 93.14$ (1)°, and $Z = 4$. A total of 5651 unique reflections with $F > 2.33\sigma(F)$ were employed, and the structure solution was refined to conventional R and R_w indices of 6.32 and 6.75, respectively. The vanadium(IV) centers are bridged by two symmetry-related $\eta^2:\eta^2\text{-}\mu_2\text{-S}_2^{2-}$ ligands, and two bidentate chelating trithiocarbonate ligands complete the coordination sphere about each metal. The metal centers are eight-coordinate, and the coordination geometry is best described as distorted dodecahedral. The V–V distances in the two independent molecules present in the unit cell are 2.872 (6) and 2.841 (6) Å, respectively, and the complex is diamagnetic. An EHMO calculation was performed in order to assess the extent of metal–metal bonding in **2**. Comparisons with the more highly developed area of Mo/S chemistry are made. The terminal trithiocarbonate sulfur atoms of **2** are nucleophilic and can be alkylated with MeI to produce the neutral compound $\text{V}_2(\text{S}_2)_2(\text{S}_2\text{CSMe})_4$ (**3**) in high yield. Compound **3** reacts with secondary amines to form the dialkylthiocarbamate compounds $\text{V}_2(\text{S}_2)_2(\text{S}_2\text{CNR}_2)_4$ ($\text{R} = \text{Et}$ (**4a**); $\text{R} = {}^n\text{Bu}$ (**4b**)). Solution-phase ^1H and ^{13}C NMR studies of dimers **2–4** indicate the presence of two isomers whose interconversion is slow on the NMR time scale. Solution-phase ^{51}V NMR data are reported for compounds **1–4** and are compared to literature values for other V/S complexes.

Introduction

We have been studying vanadium–sulfur–thiolate chemistry for a number of years because of the relevance and importance of these compounds to a wide variety of chemical, industrial, and biological systems. These complexes may serve as models for the transformation of vanadyl (VO^{2+}) impurities present in crude oils to polymeric vanadium sulfides (e.g., V_2S_3 , V_3S_4) under the reducing and sulfur-rich conditions of hydrodesulfurization.¹ The sulfides thus produced decrease the activity and lifetime of the heterogeneous catalyst employed (e.g., Mo/Co/S on alumina). Vanadium–sulfide–thiolate compounds can also be viewed as soluble, discrete structural counterparts of polymeric vanadium sulfide phases that are of interest for their magnetic and electric properties, catalytic activity, and use as electrodes in solid-state batteries.² The availability of molecular compounds allows for characterization of the reactivity and other intrinsic properties of the basic building block of the extended lattice. Furthermore, EXAFS results obtained for a vanadium-containing nitrogenase

suggest that the metal center is located in a complete or partial sulfur environment, so the study of model compounds may help delineate biochemical structural aspects and reaction pathways.³ A more basic reason to study these compounds is to explore their reactivity characteristics and compare these results to the better-developed area of molybdenum–sulfur chemistry.

In recent reports, we have described the preparation and properties of a variety of discrete vanadium–sulfide–thiolate complexes of nuclearity 1–4 and oxidation level III–V.⁴ With a number of compounds in hand, we have recently turned our attention to an exploration of the reactivity of these compounds with small organic molecules. A particularly attractive candidate for reactivity studies is the vanadium(V) monomer $(\text{Me}_3\text{NBz})_2[\text{V}(\text{S}_2)_2(\text{SPh})]$.^{4c} In addition to a variety of nucleophilic sites, the presence of an easily oxidizable thiolate in conjunction with

[†] Indiana University.

[‡] University of Hamburg.

- (1) (a) Silbernagel, B. G.; Mohan, R. R.; Singhal, G. H. *ACS Symp. Ser.* **1984**, *248*, 91. (b) Silbernagel, B. G. *J. Catal.* **1979**, *56*, 315. (c) Asaka, S.; Nakata, S.; Takeuchi, C. *ACS Symp. Ser.* **1987**, *344*, 275. (d) Rosa-Brussin, M.; Moranta, D. *Appl. Catal.* **1984**, *11*, 85. (e) Mitchell, P. C. H.; Scott, C. E.; Bonnelle, J.-P.; Grimblot, J. G. *J. Chem. Soc., Faraday Trans. 1* **1985**, *81*, 1047.
- (2) (a) Hullinger, F. *Struct. Bonding (Berlin)* **1968**, *4*, 83. (b) Whittingham, M. S. *J. Electrochem. Soc.* **1976**, *123*, 315. (c) Weissner, O.; Landa, S. *Sulfide Catalysts: Their Properties and Applications*; Pergamon: New York, 1973. (d) Rouxel, J.; Brec, R. *Annu. Rev. Mater. Sci.* **1986**, *16*, 137.

- (3) (a) Robson, R. L.; Eady, R. R.; Richardson, T. H.; Miller, R. W.; Hawkins, M.; Postgate, J. R. *Nature (London)* **1986**, *322*, 388. (b) Hales, B. J.; Case, E. E.; Morningstar, J. E.; Dzeda, M. F.; Mauterer, L. A. *Biochemistry* **1986**, *25*, 7251. (c) Arber, J. M.; Dobson, B. R.; Eady, R. R.; Stevens, P.; Hasnain, S. S.; Garner, C. D.; Smith, B. E. *Nature (London)* **1987**, *325*, 372.
- (4) (a) Money, J. K.; Huffman, J. C.; Christou, G. *Inorg. Chem.* **1985**, *24*, 3297. (b) Money, J. K.; Foltz, K.; Huffman, J. C.; Collison, D.; Temperly, J.; Mabbs, F. E.; Christou, G. *Inorg. Chem.* **1986**, *25*, 4583. (c) Money, J. K.; Nicholson, J. R.; Huffman, J. C.; Christou, G. *Inorg. Chem.* **1986**, *25*, 4072. (d) Money, J. K.; Huffman, J. C.; Christou, G. *J. Am. Chem. Soc.* **1987**, *109*, 2210. (e) Money, J. K.; Foltz, K.; Huffman, J. C.; Christou, G. *Inorg. Chem.* **1987**, *26*, 944. (f) Money, J. K.; Huffman, J. C.; Christou, G. *Inorg. Chem.* **1988**, *27*, 507. (g) Christou, G.; Heinrich, D. D.; Money, J. K.; Rambo, J. R.; Huffman, J. C.; Foltz, K. *Polyhedron* **1989**, *8*, 1723. (h) Heinrich, D. D.; Foltz, K.; Huffman, J. C.; Reynolds, J. G.; Christou, G. *Inorg. Chem.* **1991**, *30*, 300.

a metal in its highest oxidation state suggests that this compound should display high reactivity. In fact, the compound is metastable in solution ($t_{1/2}$ of ca. 4 h in MeCN) and reacts with a variety of substances, including elemental S and Se, electron-deficient acetylenes, and heterocumulenes such as CS₂. The production of a vanadium(IV) dimer from the reaction between [V(S₂S₂(SPh))]²⁻ and CS₂ and subsequent reactivity studies on this dimer are the subject of the current report.

Experimental Section

Syntheses. All manipulations were performed under a purified nitrogen atmosphere employing standard Schlenk techniques and a Vacuum Atmospheres glovebox. Tetrahydrofuran, diethyl ether, and hexanes were distilled from purple sodium benzophenone ketyl. Acetonitrile and chloroform were distilled from CaH₂. Carbon disulfide, ⁿBu₂NH, Et₂NH, MeI, and DMSO were stored over activated 4-Å molecular sieves. Anhydrous VCl₃ was used as received (Aldrich). LiSPh and NaSPh were prepared by addition of the alkali metal to a THF solution containing a slight excess of PhSH; the white precipitate was collected by filtration, washed with Et₂O, and dried under vacuum.

A. (Me₃NBz)₂[V(S₂S₂(SPh))₂] (1). This material was previously synthesized in 30–40% yield.^{4c} An improved procedure uses LiSPh in place of NaSPh. Hence, to a stirred slurry of VCl₃ (1.57 g, 9.98 mmol), LiSPh (8.13 g, 70.0 mmol), and Et₄NCl (3.30 g, 19.9 mmol) in MeCN (250 mL) was added S (0.96 g, 30 mmol). The initial orange-brown solution quickly darkened upon S addition to a deep green coloration. After being stirred for 1 h, the mixture was filtered, leaving a small amount of purple precipitate and giving an intense green filtrate. Addition of Me₃NBzCl (3.70 g, 19.9 mmol), followed by Et₂O (ca. 30 mL) to the filtrate initiated crystallization of 1. After overnight storage of the flask at -10 °C, the black crystalline product was collected by filtration, washed with MeCN/Et₂O (1:3), and dried under vacuum (yield 4.13 g, 70% based on V). IR (Nujol, cm⁻¹): 1574 (m), 1312 (w), 1265 (w), 1215 (w), 1156 (w), 1078 (m), 1024 (m), 988 (w), 976 (m), 930 (w), 918 (w), 891 (m), 831 (w), 779 (m), 741 (s), 723 (s), 700 (s, sh), 694 (s, sh), 529 (vs), 496 (m), 453 (m), 421 (w). Electronic spectrum in MeCN, λ_{max}/nm (ε_m/L mol⁻¹ cm⁻¹): 206 (sh, 52 000), 230 (sh, 30 000), 296 (14 000). ⁵¹V NMR (35.1 mM in 1:1 CD₃CN/DMSO): δ +970 ppm.

B. (Me₃NBz)₂[V₂(S₂)₂(CS₃)₄] (2). To a stirred slurry of 1 (0.40 g, 0.68 mmol) in MeCN (45 mL) was added CS₂ (0.41 mL, 6.8 mmol) via syringe. The solution quickly turned deep red. After being stirred for 1 h, the mixture was filtered, leaving a small amount of brown powder and a deep red filtrate. Storage of the filtrate at ambient temperature for several days gave 2 as black crystals. Recrystallization can be effected from warm MeCN. Typical yields are 60–70%. Analysis of material dried under vacuum indicates the nonsolvated form. Anal. Calcd for C₄₄H₆₄N₄S₁₆V₂: C, 41.81; H, 5.10; N, 4.43; S, 40.59; V, 8.06. Found: C, 41.50; H, 5.28; N, 4.51; S, 41.15; V, 8.14. IR (Nujol, cm⁻¹): 1559 (w), 1215 (w), 1157 (w), 1034 (w), 990 (s), 885 (s), 779 (m), 727 (s), 702 (m), 667 (w), 613 (w), 575 (w), 517 (m), 484 (w), 453 (w), 410 (w), 360 (m). Electronic spectrum in MeCN, λ_{max}, nm (ε_m/V₂, L mol⁻¹ cm⁻¹): 206 (91 000), 242 (39 000), 290 (34 000), 336 (54 000), 490 (6200). ¹³C NMR (¹H-decoupled, DMSO-*d*₆): δ 253.0, 252.8 ppm (CS₃)₂²⁻. ⁵¹V NMR (8.8 mM in 1:7 CD₃CN/DMSO): δ +135 ppm.

C. V₂(S₂)₂(S₂CSMe)₄ (3). To a stirred slurry of 2 (0.200 g, 0.158 mmol) in MeCN (50 mL) was added MeI (60 μL, 0.96 mmol) via syringe. Over a period of 2 days, the solution became colorless and a brown precipitate was observed. This material was collected by filtration, washed with MeCN/Et₂O (1:3), and dried under vacuum (yield 0.100 mg, 88%). Anal. Calcd for C₂₀H₁₂S₁₆V₂: C, 13.29; H, 1.67; V, 14.09. Found: C, 13.32; H, 1.71; V, 13.27. IR (Nujol, cm⁻¹): 1407 (w), 1308 (w), 1159 (w), 1015 (m), 965 (s), 953 (s), 938 (s), 926 (s), 721 (m), 583 (m), 515 (m), 465 (w), 413 (w). Electronic spectrum in CHCl₃, λ_{max}, nm (ε_m/V₂, L mol⁻¹ cm⁻¹): 286 (34 000), 318 (42 000), 480 (4300). ¹H NMR (CDCl₃): δ 2.662 (s), 2.658 ppm (s). ⁵¹V NMR (8.8 mM in 1:7 CD₃CN/DMSO): δ +173 ppm.

D. V₂(S₂)₂(S₂CNR₂)₄ (R = Et (4a)). To a stirred slurry of 3 (0.400 g, 0.553 mmol) in THF (50 mL) was added HNEt₂ (0.37 mL, 3.6 mmol) via syringe. Over a period of ca. 18 h, the solution became homogeneous and dark red-brown. The solvent was removed, and the resulting dark brown material was washed with 3 × 10 mL portions of hexane. Black crystals were obtained after recrystallization from THF/hexane at -10 °C (yield 225 mg, 50%). Anal. Calcd for C₂₀H₄₀N₄S₁₂V₂: C, 29.18; H, 4.90; N, 6.80; V, 12.38. Found: C, 29.25; H, 4.98; N, 6.54; V, 12.68. IR (Nujol, cm⁻¹): 1485 (s), 1426 (s), 1354 (s), 1306 (w), 1269 (s), 1211 (m), 1140 (m), 1073 (w), 1038 (w), 1001 (w), 914 (w), 882 (w), 849 (m),

779 (m), 723 (m), 577 (w), 554 (m), 498 (w), 438 (w), 349 (m). Electronic spectrum in THF, λ_{max}, nm (ε_m/V₂, L mol⁻¹ cm⁻¹): 246 (36 000), 278 (32 000), 364 (9600), 478 (2000), 550 (1800). ¹H NMR (CDCl₃): δ 3.77 (m, 16H, CH₂), 1.24 (t, 12H, J = 6.6 Hz, CH₃), 1.16 ppm (t, 12H, J = 7.2 Hz, CH₃). ¹³C NMR (¹H-decoupled, CDCl₃): δ 44.43, 44.35, 43.99, 43.86 (CH₂), 12.74, 12.45 ppm (CH₃). ⁵¹V NMR (CDCl₃): δ +103 ppm.

E. V₂(S₂)₂(S₂CNR₂)₄ (R = Bu (4b)). To a stirred slurry of 3 (0.340 g, 0.470 mmol) in THF (50 mL) was added ⁿBu₂NH (2.4 mL, 14.2 mmol) via syringe. After 2 h, the solution became homogeneous and deep red. The solvent was removed, leaving a dark oil that was repeatedly washed with 10-mL portions of hexane until a brown powder was obtained. Recrystallization from THF/hexanes at -10 °C gave dark brown crystals (yield 210 mg, 43%). Anal. Calcd for C₃₆H₇₂N₄S₁₂V₂: C, 41.28; H, 6.93; N, 5.35. Found: C, 41.48; H, 7.19; N, 5.24. IR (Nujol, cm⁻¹): 1491 (s), 1424 (s), 1366 (s), 1304 (m), 1289 (m), 1258 (w), 1219 (s), 1183 (w), 1142 (m), 1109 (w), 1092 (w), 1049 (w), 1013 (w), 974 (w), 951 (w), 930 (w), 909 (w), 779 (w), 723 (s), 604 (m), 586 (m), 559 (w), 515 (w), 436 (w), 377 (w), 364 (m). Electronic spectrum in THF, λ_{max}, nm (ε_m/V₂, L mol⁻¹ cm⁻¹): 242 (35 000), 288 (32 000), 370 (9600), 472 (2700), 560 (1500). ¹H NMR (CDCl₃): δ 3.66 (m, 16H, NCH₂), 1.61 (m, 16H, NCH₂CH₂), 1.31 (m, 16H, NCH₂CH₂CH₂), 0.956 (t, 6H, J = 7.33 Hz, CH₃), 0.947 (t, 6H, J = 7.34 Hz, CH₃), 0.887 ppm (t, 12H, J = 7.35 Hz, CH₃). ¹³C NMR (¹H-decoupled, CDCl₃): δ 49.81, 49.69, 49.33, 49.14 (NCH₂), 29.46, 29.24 (NCH₂CH₂), 20.15, 20.06 (NCH₂CH₂CH₂), 13.83 ppm (CH₃). ⁵¹V NMR (CDCl₃): δ +101 ppm.

Other Measurements. Infrared spectra (Nujol mull) were recorded on a Nicolet 510P FTIR or on a Perkin-Elmer 283. Cyclic voltammetry experiments were performed in a nitrogen-filled glovebox using a BAS CV-27 potentiostat and an IBM Model 7424M X-Y recorder. The reference electrodes used consisted of a cracked glass bead outer shell (Fisher) containing a Ag wire in contact with a saturated solution (MeCN or THF) of AgCl/Me₄NCl. A Pt working electrode and a Pt mesh auxiliary electrode were also used. The concentration of electroactive species was ca. 2 mM with a supporting electrolyte (ⁿBu₄NPF₆) concentration of 100 mM. Potentials are referenced vs FeCp₂/FeCp₂⁺. No IR compensation was employed. The scan rate was 200 mV/s. ¹H and ¹³C NMR spectra were recorded on a Varian XL-300 (299.94 MHz, ¹H; 75.47 MHz, ¹³C) or a Bruker AM-500 (500.137 MHz, ¹H; 125.73 MHz, ¹³C) at Indiana University. Chemical shifts were referenced to the carbons or residual protons of the solvent. ⁵¹V NMR spectra (94.73 MHz) were obtained on a Bruker AM-360 spectrometer using 10 mm diameter sample tubes at the University of Hamburg. Chemical shifts were referenced to an external standard of VOCl₃ (0 ppm). UV-visible spectra were recorded on a Hewlett-Packard 8452A diode array spectrophotometer. Elemental analyses were performed by Galbraith Laboratories, Knoxville, TN.

X-ray Crystallography and Structure Solution. Data were collected on a Picker four-circle diffractometer by using standard low-temperature procedures; details of the diffractometry, low-temperature facilities, and computational procedures employed by the Molecular Structure Center are available elsewhere.^{5a} Data collection parameters are summarized in Table I. The structures were solved by a combination of direct methods (MULTAN78) and Fourier techniques and refined by full-matrix least-squares methods. No absorption correction was performed.

(Me₃NBz)₂[V(S₂S₂(SPh))₂] (1). A systematic search of a limited hemisphere of reciprocal space located a set of diffractive maxima with monoclinic symmetry and systematic absences corresponding to the unique space group P2₁/n. The positions of all hydrogen atoms were clearly visible in a difference Fourier map phased on the non-hydrogen atoms, and the coordinates and isotropic thermal parameters for hydrogens were varied in the final cycles of refinement. A final difference Fourier was essentially featureless, with the largest peak being 0.5 e/Å³.

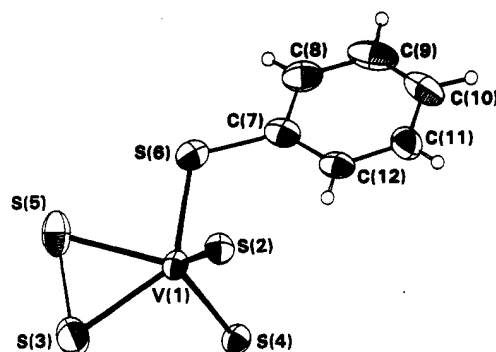
(Me₃NBz)₂[V(S₂)₂(CS₃)₄] (2). A suitable crystal was kept in contact with the mother liquor until mounted to avoid solvent loss problems noticed with earlier crystals, which were found to diffract weakly or not at all. A systematic search of a limited hemisphere of reciprocal space revealed symmetry and systematic absences corresponding to the unique monoclinic space group P2₁/c. The V and S atom positions were obtained from an initial E-map. The remainder of the non-hydrogen atoms were found in subsequent iterations of least-squares refinement and difference Fourier

- (5) (a) Chisholm, M. H.; Folting, K.; Huffman, J. C.; Kirkpatrick, C. C. *Inorg. Chem.* **1984**, *23*, 1021. (b) Ammeter, J. H.; Bürgi, H.-B.; Thibault, J. C.; Hoffmann, R. *J. Am. Chem. Soc.* **1978**, *100*, 3686. (c) Kubáček, P.; Hoffmann, R.; Haulas, Z. *Organometallics* **1982**, *1*, 180. (d) Chen, M. M. L.; Hoffmann, R. *J. Am. Chem. Soc.* **1976**, *98*, 1647. (e) Hoffmann, R. *J. Chem. Phys.* **1963**, *39*, 1397.

Table I. Crystallographic Data for Complexes 1 and 2

parameters	1	2
formula	C ₂₆ H ₁₇ N ₂ S ₅ V	C ₄₆ H ₆₇ N ₅ S ₁₆ V ₂
molar mass, g mol ⁻¹	588.85	1304.91
cryst syst	monoclinic	monoclinic
space group	P2 ₁ /n	P2 ₁ /c
temp, °C	-158	-114
a, Å	18.178 (8) ^a	20.978 (4) ^b
b, Å	8.843 (2)	13.384 (2)
c, Å	18.852 (7)	21.613 (4)
β, deg	107.06 (2)	93.14 (1)
Z	4	4
V, Å ³	2897.16	6059.27
radiation, Å	0.710 69	0.710 69
abs coeff, cm ⁻¹	6.951	8.643
R, % ^c	5.65	6.32
R _w , % ^d	5.63	6.75

^a 34 reflections. ^b 50 reflections. ^c $R = \sum ||F_o| - |F_c|| / \sum |F_o|$. ^d $R_w = [\sum w(|F_o| - |F_c|)^2 / \sum w|F_o|^2]^{1/2}$, where $w = 1/\sigma^2(|F_o|)$.

**Figure 1.** ORTEP representation of the anion of complex 1 at the 50% probability level.

calculations. After partial refinement of the non-hydrogen atoms, a difference Fourier map revealed some, but not all, hydrogen atoms. All hydrogen atoms except those of the MeCN solvate molecule were introduced in fixed calculated positions. In the final cycles of least-squares refinement, all non-hydrogen atoms were varied with anisotropic thermal parameters. A final difference Fourier map was featureless, with the largest peak being 0.99 e/Å³.

Molecular Orbital Calculations. Calculations were performed using the EHMO method with weighted H_{ij} 's.^{5b} The parameters for V,^{5c} S,^{5d} and C^{5e} were taken from the literature. Atomic coordinates were taken from the crystallographic data.

Results and Discussion

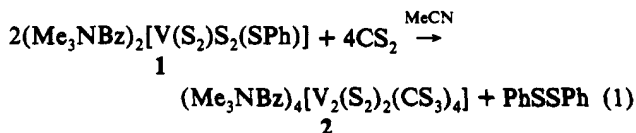
Syntheses and Structures. The original synthesis of [V(S₂)S₂(SPh)]²⁻ (1) was plagued with concomitant formation of a purple oligomeric material of as-yet undetermined formulation.^{4c} We have since discovered that replacement of NaSPh with LiSPh in a reaction mixture comprising VCl₃, LiSPh, S, and NEt₄Cl in a 1:7:3:2 molar ratio in MeCN avoids the formation of the purple material and increases the yield of 1 from ca. 35% to ca. 65%. The material crystallizes directly from the reaction solution in a form suitable for crystallography. Table II lists atomic coordinates, and Figure 1 shows an ORTEP representation of the anionic portion of compound 1. Selected bond distances and angles are listed in Table III. The vanadium(V) center is ligated by three types of sulfur atoms, viz. one PhS⁻, one persulfido (S₂²⁻), and two sulfido (S²⁻) groups, yielding a VS₅ core of idealized C_s symmetry. The coordination geometry is best described as tetrahedral with the S₂²⁻ considered as occupying one site. Although many vanadium(III or IV)/thiolate linkages are known,^{4a,6,7} compound 1 is the only structurally-characterized

Table II. Selected Fractional Coordinates (×10⁴) and Isotropic Thermal Parameters (Å² × 10) for Complexes 1 and 2

atom	x	y	z	B _{iso}
Complex 1				
V1	9226 (1)	1923 (1)	1687 (1)	20
S2	9948 (1)	2043 (2)	1005 (1)	24
S3	9958 (1)	3049 (2)	2802 (1)	38
S4	9119 (1)	-305 (2)	2027 (1)	23
S5	8995 (1)	4151 (2)	2239 (1)	35
S6	7965 (1)	2384 (2)	907 (6)	28
Complex 2				
V1	272 (1)	979 (1)	4953 (1)	15
V2	5452 (1)	677 (1)	9771 (1)	16
S3	406 (1)	-141 (2)	5813 (1)	21
S4	-477 (1)	445 (2)	5707 (1)	18
S5	713 (1)	2237 (2)	5711 (1)	23
S6	1459 (1)	931 (2)	5034 (1)	22
S7	505 (1)	2156 (2)	4097 (1)	24
S8	-575 (1)	2291 (2)	4804 (1)	23
S9	-560 (1)	3556 (2)	3662 (1)	37
S10	2126 (1)	2011 (2)	6090 (1)	32
S11	5633 (1)	-445 (2)	10644 (1)	20
S12	5039 (1)	704 (2)	10787 (1)	21
S13	5773 (1)	1251 (2)	8744 (1)	23
S14	6448 (1)	-188 (2)	9463 (1)	24
S15	5044 (1)	2428 (2)	9756 (1)	21
S16	6278 (1)	1869 (2)	10201 (1)	20
S17	5934 (1)	4070 (2)	10179 (1)	25
S18	6872 (1)	236 (2)	8173 (1)	37
C23	1461 (4)	1757 (7)	5634 (4)	22
C24	-228 (4)	2729 (7)	4152 (4)	21
C25	6392 (5)	415 (7)	8750 (5)	27
C26	5764 (5)	2857 (7)	10062 (5)	25

complex with this linkage at the +5 metal oxidation state. The V-S6-C7 angle of 111.67 (24)° is very close to that found in vanadium(III)/benzenethiolate compounds.⁷ Unlike the case of alkoxides, this angle is not indicative of the amount of metal-sulfur d-π-p-π bonding, since the sulfur 3p orbital is oriented perpendicular to the M-S-C plane.⁸ The S-S bond length in the S₂²⁻ ligand of 2.013 (3) Å is typical⁹ for bound persulfide and is consistent (vide infra) with ligand π* to empty metal d-orbital electron donation (free S₂²⁻; S-S = 2.13 Å).¹⁰ The V-S2 and V-S4 distances of 2.092 (2) and 2.099 (2) Å are somewhat shorter than those in VS₄³⁻ (2.135–2.175 (1) Å),¹¹ the only other known vanadium(V) monomer with terminal sulfide ligation.

The unusual nature of 1, particularly the V^V/PhS⁻ linkage, suggested that it might be highly reactive, and we have therefore investigated its reactions with, among other things, carbon disulfide. Addition of excess CS₂ to an MeCN solution of compound 1 rapidly formed a deep red color. Following filtration, well-formed crystals of 2 grew slowly from this solution at ambient temperature in good yield. Elemental analysis indicated two cations and eight sulfur atoms per vanadium. The formula and nuclearity of this product were determined by X-ray crystallography to be (Me₃NBz)₄[V₂(S₂)₂(CS₃)₄] (2). The formation of 2 can be summarized as shown in eq 1. Oxidation of the thiolate



in compound 1 to the disulfide provides for concomitant reduction of vanadium(V) to vanadium(IV).

The crystallographic study of 2 revealed two independent molecules in the unit cell with each dimeric molecule residing on

- (6) (a) Fachinetti, G.; Floriani, C. *J. Chem. Soc., Dalton Trans.* 1974, 2433. (b) Wiggins, R. W.; Huffman, J. C.; Christou, G. *J. Chem. Soc., Chem. Commun.* 1983, 1313. (c) Dorfman, J. R.; Holm, R. H. *Inorg. Chem.* 1983, 22, 3179. (d) Szymles, D.; Krebs, B.; Henkel, G. *Angew. Chem., Suppl.* 1983, 1176.

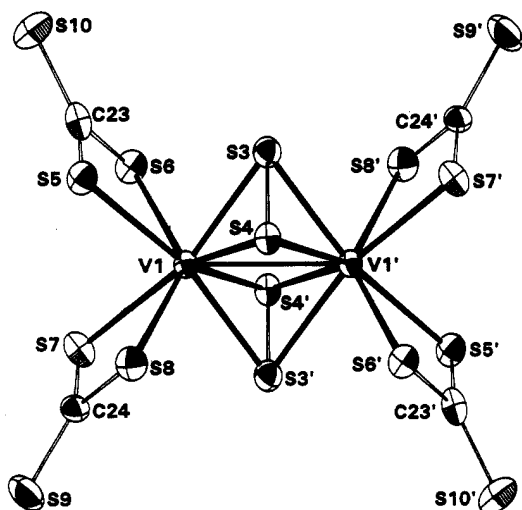
- (7) Dean, N. S.; Christou, G. Unpublished results.

- (8) Ashby, M. T. *Comments Inorg. Chem.* 1990, 10, 297. (9) Gambarotta, S.; Floriani, C.; Chiesi-Villa, A.; Guastini, C. *J. Chem. Soc., Chem. Commun.* 1983, 184. (10) Coucouvanis, D.; Hadjikyriacou, A.; Draganjac, M.; Kanatzidis, M. G.; Ilperuna, O. *Polyhedron* 1986, 5, 349. (11) Do, Y.; Simhon, E. D.; Holm, R. H. *Inorg. Chem.* 1985, 24, 4635.

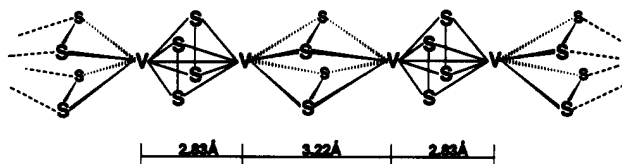
Table III. Selected Distances (Å) and Angles (deg) for Complexes 1 and 2

Complex 1			
V1–S2	2.0919 (20)	V1–S6	2.3674 (23)
V1–S3	2.3549 (23)	S3–S5	2.013 (3)
V1–S4	2.0988 (20)	S6–C7	1.765 (7)
V1–S5	2.3230 (23)		
S2–V1–S3	103.57 (9)	S4–V1–S5	127.88 (8)
S2–V1–S4	111.52 (8)	S4–V1–S6	101.08 (8)
S2–V1–S5	117.40 (8)	S5–V1–S6	82.11 (8)
S2–V1–S6	106.14 (8)	V1–S3–S5	63.70 (8)
S3–V1–S4	101.69 (8)	V1–S5–S3	65.33 (9)
S3–V1–S5	50.97 (8)	V1–S6–C7	111.67 (24)
S3–V1–S6	132.24 (8)		
Complex 2 ^a			
V1–V1'	2.8720 (59)	V2–V2'	2.8411 (57)
V1–S3	2.3930 (28)	V2–S11	2.4205 (27)
V1–S3'	2.4009 (28)	V2–S11'	2.4258 (27)
V1–S4	2.4324 (27)	V2–S12	2.406 (3)
V1–S4'	2.4325 (27)	V2–S12'	2.4070 (28)
V1–S5	2.492 (3)	V2–S13	2.476 (3)
V1–S6	2.4859 (27)	V2–S14	2.510 (3)
V1–S7	2.4973 (28)	V2–S15	2.4949 (28)
V1–S8	2.5069 (28)	V2–S16	2.4968 (27)
S3–S4	2.012 (3)	S11–S12	2.014 (3)
S3–V1–S3'	106.39 (9)	S4–V1–S7	147.26 (10)
S3'–V1–S4	86.79 (9)	S4–V1–S8	79.15 (9)
S3–V1–S4	49.29 (8)	S4'–V1–S8	128.35 (10)
S3–V1–S4'	86.97 (9)	S5–V1–S6	68.72 (9)
S3'–V1–S4'	49.20 (8)	S5–V1–S7	88.92 (10)
S3–V1–S5	83.59 (9)	S5–V1–S8	81.16 (9)
S3'–V1–S5	162.51 (10)	S6–V1–S7	80.44 (9)
S3–V1–S6	81.60 (9)	S6–V1–S8	136.72 (10)
S3'–V1–S6	126.15 (10)	S7–V1–S8	68.27 (9)
S3–V1–S7	162.01 (10)	V1–S3–V1'	73.61 (9)
S3'–V1–S7	85.24 (9)	V1–S3–S4	66.38 (10)
S3'–V1–S8	81.36 (9)	V1–S3'–S4	66.22 (10)
S3–V1–S8	126.17 (10)	V1–S4–V1'	72.36 (8)
S4–V1–S4'	107.64 (8)	V1–S4'–S3	64.58 (10)
S4–V1–S5	89.28 (9)	V1–S4–S3	64.34 (10)
S4'–V1–S5	147.56 (10)	V1–S5–C23	89.5 (3)
S4–V1–S6	128.71 (10)	V1–S6–C23	89.9 (3)
S4'–V1–S6	79.24 (9)	V1–S7–C24	91.0 (3)
S4'–V1–S7	90.72 (9)	V1–S8–C24	90.8 (3)

^a Only limited data are listed for the second independent anion (V2, V2'); full listings are available in the supplementary material.

**Figure 2.** ORTEP representation of the anion of complex 2 at the 50% probability level.

an inversion center. An ORTEP projection of one of the independent anions is shown in Figure 2; atomic coordinates and structural parameters are listed in Tables II and III, respectively. The metal centers are bridged by two symmetry-related $\eta^2\text{-}\eta^2\text{-}\mu_2\text{-S}_2^2$ ligands, and two bidentate chelating trithiocarbonate ligands

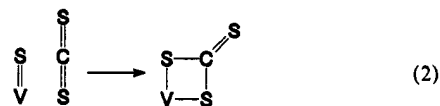
**Figure 3.** Portion of the infinite linear chain present in the mineral patronite.**Table IV.** Comparison of Core Distances in $\text{V}_2(\text{S}_2)_2\text{Z}_4$

	Z				patronite, [V(S ₂) ₂] _n
	(CS ₃) ₂ ²⁻	(S ₂ CN ⁱ Bu ₂) ⁻	(S ₂ CNEt ₂) ⁻	(S ₂ CCH ₃) ⁻	
V–V'	2.872	2.851	2.884	2.800	2.83
V–S(av)	2.415	2.405	2.409	2.392	2.41
S–S	2.012	1.998	1.984	1.997	2.03
ref	a	12	14	13	15

^a This work.

complete the coordination sphere about each vanadium. The metal centers are eight-coordinate, and the coordination geometry is best described as distorted dodecahedral. The V–V distances in the two independent molecules are 2.872 (6) and 2.841 (6) Å, respectively, which is within bonding range (*vide infra*). Similar $[\text{V}_2(\text{S}_2)_2]^{4+}$ cores have been observed in the molecular compounds $\text{V}_2(\text{S}_2)_2(\text{S}_2\text{CN}^i\text{Bu}_2)_4$,¹² $\text{V}_2(\text{S}_2)_2(\text{S}_2\text{CMe})_4$,¹³ and $\text{V}_2(\text{S}_2)_2(\text{S}_2\text{CNEt}_2)_4$.¹⁴ These complexes, including 2, are all related to the polymeric, solid-state mineral known as patronite. The latter consists of linear chains of vanadium(IV) ions bridged by two S_2^{2-} ligands, as illustrated in Figure 3.¹⁵ The metal centers in patronite have pairwise bonding interactions (2.83 Å) and longer, nonbonding distances (3.22 Å). A comparison of these core distances is tabulated in Table IV.

The rapidity of the reaction and lack of suitable monitoring techniques make it difficult to deduce the mechanism of the conversion of 1 to 2. Of particular interest would be the initial site of attack of CS_2 on the $[\text{V}(\text{S}_2)_2(\text{SPh})]^{2-}$ anion. Given the retention of the V:S₂²⁻ ratio (1:1) of 1 in the product 2 and the loss of terminal sulfides, it is tempting to postulate attack of CS_2 at the VS groups to directly give chelating CS_3^{2-} groups via [2+2] cycloaddition (eq 2). Although rare, such cycloaddition reactions



involving $\text{M}=\text{X}$ ($\text{X} = \text{O}, \text{S}$) are known. For example, $(\text{CF}_3)_2\text{C}=\text{O}$ cycloadds¹⁶ across the $\text{W}=\text{O}$ group of $\text{Cp}_2\text{W}=\text{O}$ and, in a similar fashion, SO_2 cycloadds across a $\text{Re}=\text{O}$ bond on each Re atom of $\text{Cp}^*\text{Re}_2\text{O}_4$.¹⁷ Most recently, the complex $(\text{tmtaa})\text{Ti}=\text{O}$ has been shown to undergo many [2+2] cycloadditions with a number of reagents such as ketones, SO_2 , SO_3 , and CS_2 . Similarly, the thio complex $(\text{tmtaa})\text{Ti}=\text{S}$ is reported to react with CS_2 to give $(\text{tmtaa})\text{Ti}(\text{CS}_3)$.¹⁸ Thus, the reaction of 1 with CS_2 might also be proceeding via a cycloaddition reaction with the terminal $\text{V}=\text{S}$ groups; major loss of the π -donation to the metal from these multiply-bonded S_2^{2-} groups would then trigger both reduction of the metal by the PhS^- group and

(12) Halbert, T. R.; Hutchings, L. L.; Rhodes, R.; Stiefel, E. I. *J. Am. Chem. Soc.* **1986**, *108*, 6437.

(13) Duraj, S. A.; Andras, M. T.; Kibala, P. A. *Inorg. Chem.* **1990**, *29*, 1232.

(14) Yang, Y.; Huang, L.; Liu, Q.; Kang, B. *Acta Crystallogr.* **1991**, *C47*, 2085.

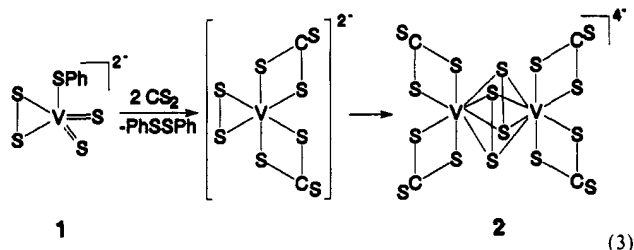
(15) (a) Allmann, R.; Baumann, I.; Kutoglu, A.; Rösch, H.; Hellner, E. *Naturwissenschaften* **1964**, *51*, 263. (b) Klemm, W.; Schnering, H. B. *Naturwissenschaften* **1965**, *52*, 12.

(16) Pilato, R. S.; Housmekerides, C. E.; Jernakoff, P.; Rubin, D.; Geoffroy, G. L.; Rheingold, A. L. *Organometallics* **1990**, *9*, 2333.

(17) Herrmann, W. A.; Jung, K. A.; Hardtweck, E. *Chem. Ber.* **1989**, *122*, 2041.

(18) Housmekerides, C. E.; Pilato, R. S.; Geoffroy, G. L.; Rheingold, A. L. *J. Chem. Soc., Chem. Commun.* **1991**, 563.

aggregation via conversion of terminal S_2^{2-} groups into bridging modes (eq 3). Alternatively, it cannot be ruled out that the CS_2



is attacking at other sites on the $[V(S_2)_2(SPh)]^{2-}$ ion, most obviously the S_2^{2-} group, and that internal electron redistribution then oxidizes the S^{2-} groups to S_2^{2-} , which adopts the bridging mode in **2**. However, this possibility should initially generate a CS_4^{2-} unit that would then have to transfer a sulfur atom to either a second CS_2 or a S^{2-} . At the very least, this mechanism would be more complex. Unfortunately, we do not have access to suitable derivatives of **1** (e.g., containing the $[V(S_2)O_2(SPh)]^{2-}$ ion) to probe this matter further.

Extended Hückel Molecular Orbital Calculations. Both $V_2(S_2)(S_2CN^iBu_2)_4$ and $V_2(S_2)_2(S_2CMe)_4$ were reported to be diamagnetic,^{12,13} as is $[V_2(S_2)_2(CS_3)_4]^{4-}$ on the basis of its 1H , ^{13}C , and ^{51}V NMR spectra (vide infra). In an effort to address the extent of metal-metal bonding in **2** (as opposed to strong antiferromagnetic coupling via the bridging ligands), EHMO calculations have been performed on the $[V_2(S_2)_2(CS_3)_4]^{4-}$ ion. (Calculations have previously been reported on "CpMS₄MCp" systems employing metal fragments of C_{3v} symmetry.¹⁹) Of the coordinates of two independent molecules present in the unit cell of **2**, the (nonidealized) coordinates of the one with the long vanadium-vanadium distance were used. The bridging persulfides were treated as one fragment and the two " $V(CS_3)_2$ " units were viewed as distorted ML_4 fragments with C_{2v} symmetry.²⁰ Symmetry labels were assigned according to the D_{2h} symmetry of the entire molecule. As shown in Figure 4, there is a metal-based orbital match for each of the persulfide π and π^* orbitals. This match leads to a good interaction between the two fragments and a large HOMO/LUMO gap (ca. 1.2 eV); the HOMO possesses approximately 13% metal 3d character. Significant electron density is transferred from the high-lying persulfide π^* orbitals to empty metal-based orbitals, thus decreasing the S-S bond distance (2.012 (3) Å in **2** vs 2.13 Å in free S_2^{2-}).¹⁰ In regard to a metal-metal σ bond, there is a greater amount of electron density transferred from the lower lying persulfide π orbitals into the metal-metal bonding, d_{z^2} combination (σ) than is transferred into the out-of-phase (σ^*) d_{z^2} combination. These results lend support for the existence of a weak metal-metal bond, although it should be noted that there is extensive mixing of sulfur character into this molecular orbital. Indeed, many quadruply- and triply-sulfur-bridged early-transition-metal compounds possess a formal metal-metal bond.¹⁹

Comparisons with Mo/S Systems. It has always been of interest to compare results obtained in our V/S studies with those available from better-understood Mo/S chemistry. Coucouvanis and co-workers have shown that the $Mo-\eta^2-S_4$ group present in both the molybdenum(IV) monomer $[(S_4)_2Mo=S]^{2-}$ and the molybdenum(V) dimer $[Mo_2S_4(S_4)_2]^{2-}$ is in equilibrium with the $Mo-\eta^2-S_2$ (persulfide) group and elemental sulfur, as shown in eqs 4 and 5.²¹ The reaction chemistry of the $Mo-\eta^2-S_4$ group is dominated by the presence of the $Mo-\eta^2-S_2$ group. Since the $[(S_4)Mo(S)(S_2)]^{2-}$ and $[(S_4)Mo_2S_4(S_2)]^{2-}$ compounds contain

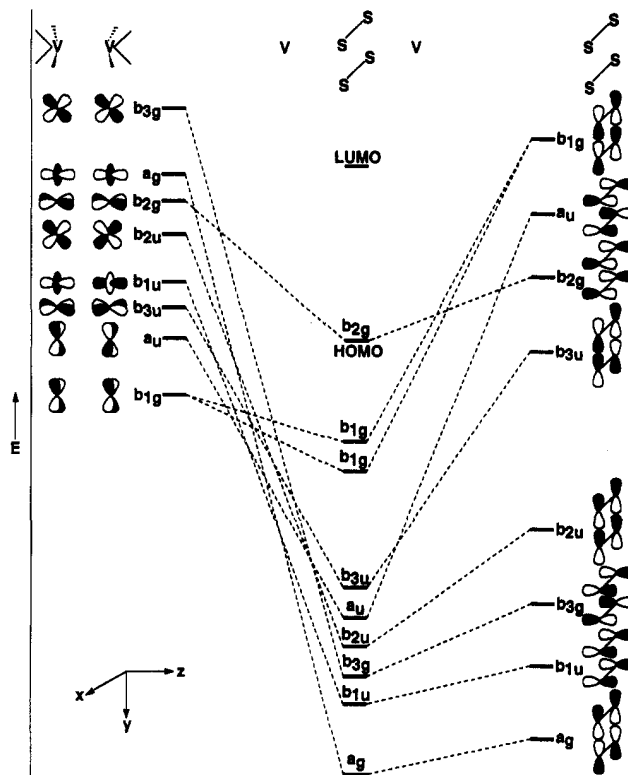
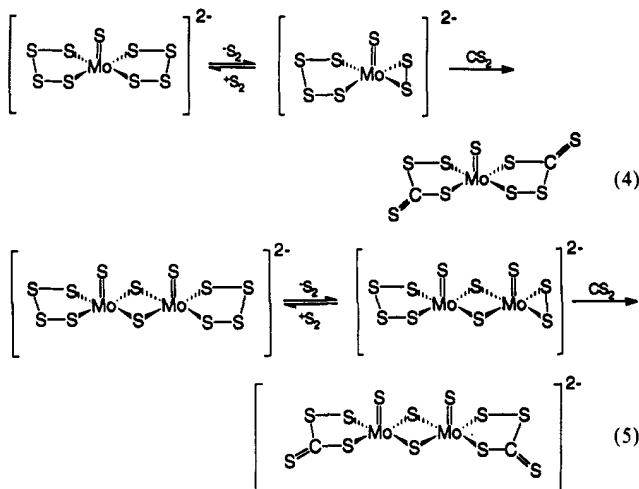


Figure 4. Interaction diagram for $[V_2(S_2)_2(CS_3)_4]^{4-}$ (anion of **2**). Labels are for D_{2h} symmetry.



structural elements²² in common with the vanadium(V) monomer $[V(S_2)_2(SPh)]^{2-}$ (terminal sulfido and persulfido), it is of interest to compare their reactivity characteristics. Both of the molybdenum species react with CS_2 to form " $(CS_4)^{2-}$ " units as shown in eqs 4 and 5.^{10,23} It should be emphasized that the $Mo-\eta^2-S_2$ unit is not "pure" in the sense that it is in equilibrium with the $Mo-\eta^2-S_4$ group and it is not known with which species the CS_2 reacts. Another possibility is that CS_2 undergoes cycloaddition with the $Mo=S$ unit followed by intramolecular S addition, forming the perthiocarbonate ligand.^{23b} However, it is apparent in both cases that the terminal sulfido group *appears* not to react and is retained in the structure of the product. The different reactivity pattern observed with the vanadium species may be due to greater nucleophilicity of a thiovanadyl unit; i.e., the $V=S$ group is more reactive toward electrophiles than the $Mo=S$ group.

(19) Tremel, W.; Hoffmann, R.; Jemmis, E. D. *Inorg. Chem.* **1989**, *28*, 1213.

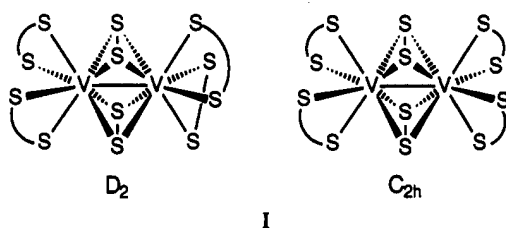
(20) Albright, T. A.; Burdett, J. K.; Whangbo, M. H. *Orbital Interactions in Chemistry*; Wiley: New York, 1985; pp 358.

(21) Coucouvanis, D.; Toupadakis, A.; Koo, S.-M.; Hadjikyriacou, A. *Polyhedron* **1989**, *8*, 1705.

(22) Draganjac, M.; Simhon, E.; Chan, L. T.; Kanatzidis, M.; Baenziger, N. C.; Coucouvanis, D. *Inorg. Chem.* **1982**, *21*, 3321.

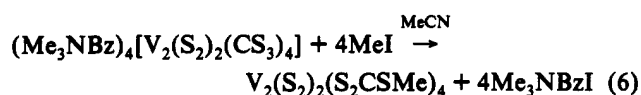
(23) (a) Coucouvanis, D.; Draganjac, M. *J. Am. Chem. Soc.* **1982**, *104*, 6820. (b) Coucouvanis, D.; Draganjac, M.; Koo, S. M.; Toupadakis, A.; Hadjikyriacou, A. *Inorg. Chem.* **1992**, *31*, 1186.

Spectroscopic Properties and Reactivity Characteristics of $[V_2(S_2)_2(CS_3)_4]^{4-}$ (2). The 1H NMR spectrum of complex 2 in CD_3CN displays only sharp signals for the Me_3NBz^+ cations at the expected chemical shifts, in accord with a diamagnetic nature for 2. In the $^{13}C\{^1H\}$ NMR spectrum, there are the expected peaks for the cation and two peaks of comparable intensity at 253.0 and 252.8 ppm assigned to the carbon atoms of two inequivalent CS_3^{2-} groups. This was an unexpected observation. The $[V_2(S_2)_2(CS_3)_4]^{4-}$ anion has virtual C_{2h} symmetry, and one would expect only a single CS_3^{2-} ^{13}C NMR signal in solution. Twice as many signals as expected were also observed in the spectra of derivatives of 2 (vide infra) and it appeared that there was probably a common explanation. We believe this explanation to be that there are two isomers in solution and that their interconversion is slow on the NMR time scale, giving multiple signals. Thus, on dissolution of the C_{2h} solid-state structure, an equilibrium is established in which the D_2 isomer is also present. The two isomers differ only in the relative orientation of the CS_3^{2-} chelates at the two ends of the molecule; the essence of this difference is indicated in simplified form in I. Each isomer of



2 should give a single ^{13}C resonance, resulting in the two observed signals of similar chemical shift. The interconversion could readily occur by, for example, partial dissociation of CS_3^{2-} groups to monodentate modes followed by reattachment. Given the expected lability of an eight-coordinate VI^V complex, it is reasonable that two isomers should exist in solution. Indeed, we note that $V_2(S_2)_2(S_2CN^iBu)_4$ crystallizes in the D_2 isomeric form, with the molecule lying on a crystallographic 2-fold rotation axis.¹² Thus, both isomers have been demonstrated to be possible. It is therefore conceivable that all members of this family of $[V_2(S_2)_2]^{4-}$ -containing species might exist in isomeric forms in solution with the solid-state form dictated by lattice energies, kinetics of crystallization, and the space group of the crystal phase. Complex 2, remember, crystallizes in $P\bar{1}$ with the anion on an inversion center, dictating the C_{2h} isomer. As previously observed in other trithiocarbonate-containing compounds,²⁴ 2 exhibits strong absorptions at 990 and 885 cm^{-1} assigned to the $\nu(C=S)$ and $\nu(C-S)$ stretching vibrations, respectively.

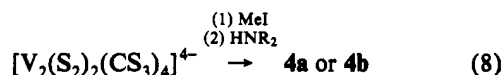
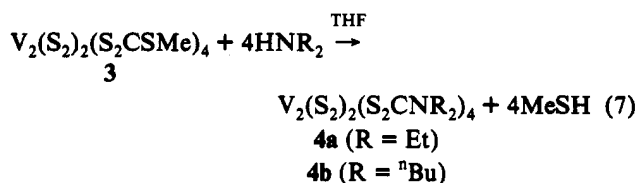
Previous work has demonstrated that the terminal sulfur of a metal-bound trithiocarbonate complex is nucleophilic and can react with alkyl halides.^{24c,d,25} Addition of excess MeI to an MeCN solution of 2 readily yields the methylated product 3 (as summarized in eq 6), which can be obtained in excellent yield



and analytical purity. The 1H NMR spectrum of 3 in $CDCl_3$ shows two sharp singlets of comparable intensity at 2.662 and 2.658 ppm, in contrast to the single resonance expected simply from methylation of the solid-state structure. This is again

consistent with two isomers being present in solution. Compound 3 also exhibits IR absorptions similar to other bound alkyl trithiocarbonates,^{24c,d,f,25,26} with the major band occurring at 965 cm^{-1} .

Alkyl trithiocarbonate compounds are known to undergo nucleophilic substitution reactions with amines to form dithiocarbamate compounds with concomitant elimination of the thiol.^{24a,d,27} We have found complex 3 to undergo similar chemistry. Thus, 3 reacts with secondary amines in THF to give the corresponding dialkyldithiocarbamate (eq 7). The structures of these compounds have been discussed above. Alternatively, compounds 4a and 4b can be prepared directly from compound 2 via sequential additions of MeI and the amine, as shown in eq 8. The coplanarity of the six atoms ($S_2C=NC_2$) of a dialkyl-



dithiocarbamate group and absence of rotation about the $C=N$ double bond cause the methylene protons of the ethyl derivative 4a to be diastereotopic. Thus, the 1H NMR spectrum of 4a in $CDCl_3$ exhibits a complex multiplet at ca. 3.7 ppm. When the methyl protons are decoupled, there are still complications from second-order effects, and so we resorted to the ^{13}C spectrum. As expected by now, four (instead of two) different ^{13}C chemical shifts are observed from the methylene carbons in the $^{13}C\{^1H\}$ NMR spectrum of 4a, consistent with the presence of two isomers. The methyl region shows only two resonances, suggesting accidental overlap. High-temperature 1H NMR spectra of compound 4a in $CDCl_3$ remained unchanged up to 70 $^{\circ}C$, the point at which decomposition began to occur. This observation suggests interconversion between the C_{2h} and D_2 isomers is still slow on the NMR time scale even at 70 $^{\circ}C$. Infrared spectra of the dithiocarbamate dimers 4a and 4b display strong absorptions at ca. 1490 cm^{-1} , in accord with other metal dialkyldithiocarbamate complexes.^{24c,d,27}

Electrochemistry. The electrochemical behavior of compounds 1–4 was investigated using cyclic voltammetry. None of the complexes exhibited any reversible features. For compound 1, cathodic scans in MeCN revealed an irreversible process at -1.7 V. Under similar conditions, compound 2 gave an irreversible wave at -2.2 V. Cathodic scans of compound 3 in THF exhibited peaks at -0.86 , -1.18 , and -1.88 V; no corresponding oxidation peaks were observed on the return scan. An anodic scan of compound 4a in THF revealed peaks at -0.42 and 0.36 V with additional peaks at 0.33 and -0.32 V observed upon the return scan. Similarly, compound 4b exhibited a peak at 0.082 V upon anodic scanning, with a peak at 0.22 V observed during the return scan.

Solution ^{51}V NMR Results. ^{51}V chemical shifts of complexes 1–4 are listed in Table V, together with data from the literature for comparison. Figure 5 is a stack plot of selected spectra.

- (24) (a) Fackler, J. P.; Seidel, W. C. *Inorg. Chem.* **1969**, *8*, 1631. (b) Burke, J. M.; Fackler, J. P. *Inorg. Chem.* **1972**, *11*, 2744. (c) Benson, I. B.; Hunt, J.; Knox, S. A. R.; Oliphant, V. J. *Chem. Soc., Dalton Trans.* **1978**, 1240. (d) Bianchini, C.; Mealli, C.; Meli, A.; Scapacci, G. *J. Chem. Soc., Dalton Trans.* **1982**, 799. (e) Bianchini, C.; Innocenti, P.; Meli, A. *J. Chem. Soc., Dalton Trans.* **1983**, 1777. (f) Aggarwal, R. C.; Singh, N.; Singh, S. *Synth. React. Inorg. Met.-Org. Chem.* **1986**, *16*, 155.
- (25) Hunt, J.; Knox, S. A. R.; Oliphant, V. J. *Organomet. Chem.* **1974**, *80*, C50.

- (26) (a) Bruce, R.; Knox, G. R. *J. Organomet. Chem.* **1966**, *6*, 67. (b) Pelizzi, G. C. *Inorg. Chim. Acta* **1970**, *4*, 618. (c) Hyde, J.; Venkatasubramanian, K.; Zubieta, J. *Inorg. Chem.* **1978**, *17*, 414.
- (27) Bradley, D. C.; Rendall, I. F.; Sales, K. D. *J. Chem. Soc., Dalton Trans.* **1973**, 2228.
- (28) Harrison, A. T.; Howarth, O. W. *J. Chem. Soc., Dalton Trans.* **1986**, 1405.
- (29) Preuss, F.; Noichl, A. Z. *Naturforsch., B* **1987**, *42*, 121.
- (30) Herberhold, M.; Kuhnlein, M.; Schrepfermann, M.; Ziegler, M. L.; Nuber, B. *J. Organomet. Chem.* **1990**, *398*, 259.
- (31) Rehder, D.; Weidemann, C.; Duch, A.; Pribsch, W. *Inorg. Chem.* **1988**, *27*, 584.

Table V. ^{51}V NMR Shifts (Relative to VOCl_3) for 1–4 and for Selected Complexes from the Literature

complex	solvent	$\delta(^{51}\text{V})$, ppm	ref
$[\text{V}_2\text{S}_6(\mu\text{-S})]^{4-}$	H_2O	+1457	28
$[\text{VS}_3\text{SH}]^{2-}$	H_2O	+1392	28
$[\text{VS}(\text{SSiPh}_3)_3]$	$\text{C}_7\text{H}_8/\text{Me}_2\text{CO}$	+1410	29
$[\text{Cp}^*\text{V}_2(\mu\text{-S})_3]$	THF	+1630	30
$[\text{Cp}^*\text{V}_2(\mu\text{-S})(\mu\text{-S}_2)_2]$	THF	+596	30
$[\text{VO}(\text{OH})(\text{S}_2\text{CNEt}_2)_2]$	CDCl_3	-468	31
$[\text{VS}_2(\text{S}_2\text{SPh})]^{2-}$ (anion of 1)	DMSO/ CD_3CN (1:1)	+970 ^a	b
$[\text{V}_2(\text{S}_2\text{CS})_4(\mu\text{-S}_2)_2]^{4-}$ (anion of 2)	DMSO/ CD_3CN (1:1)	+125	b
	DMSO/ CD_3CN (7:1)	+135	b
$[\text{V}_2(\text{S}_2\text{CZ})_4(\mu\text{-S}_2)_2]$ Z = SMe (3)	DMSO/ CD_3CN (7:1)	+173 ^c	b
Z = NEt (4a)	CDCl_3	+103	b
Z = N ⁿ Bu (4b)	CDCl_3	+101	b
$[\text{VO}_2(\text{OH})]^{2-}$	H_2O	-537	32
$[\text{VO}_2(\text{O}_2)\text{OH}]^{2-}$	H_2O	-623	32
$[\text{VO}_2(\text{dipic})]^-$	H_2O	-529	33
$[\text{VO}(\text{O}_2)\text{dipic}]^-$	H_2O	-595	33
$[\text{VO}(\text{ONH}_2)\text{dipic}]$	H_2O	-672	33

^a Two additional signals are observed at -385 and -414 ppm (see Figure 5), possibly corresponding to vanadium complexes where most of the thio ligands are replaced by DMSO and/or acetonitrile. From the relation between $\delta(^{51}\text{V})$, the ligand electronegativity, and the coordination number,^{31,34} possible compositions are $\text{V}(\text{O}/\text{N})_x\text{S}$, where $x = 5, 4$, or 3.
^b This work. ^c Prepared from 2 in DMSO/ CD_3CN by addition of a 10-fold molar excess of MeI.

Line widths of ^{51}V NMR signals of diamagnetic vanadium complexes in solution are dominated by the quadrupole relaxation mechanism (^{51}V : 99.78% natural abundance, $I = 7/2$, $Q = -0.04 \times 10^{-28} \text{ m}^2$, relative receptivity ($^1\text{H} = 1$) = 0.38) and hence depend on, inter alia, the local symmetry, the size and bulkiness of the complex, the electronic nature of the ligand, and the viscosity of the solution. In compounds 1–4, $W_{1/2}$ values are typically around 0.7 kHz, which corresponds to relaxation times in the millisecond range. The fact that the V(IV) complexes 2–4 show relatively sharp signals indicates that there is strong coupling between the two metal centers (negligible population of a triplet spin state), thus supporting the EHMO calculation results discussed previously. In contrast to the ^1H and ^{13}C spectra, no resolution of more than one peak is observed.

In compounds 1–4, the ^{51}V nucleus is deshielded with respect to VOCl_3 , the standard adopted in ^{51}V NMR spectroscopy, and also with respect to all common V(V) complexes containing oxygen and/or nitrogen ligands in the coordination sphere. As a d^0 system, the V(V) complex 1 exhibits the so-called "inverse polarizability (electronegativity) dependence of metal shielding",^{31,34,35} i.e., shielding decreases as the polarizability of the ligand function increases (or its electronegativity decreases). Hence, generally speaking, sulfur ligands give rise to low shielding, as documented by the shift values of our complexes and the other thiovanadium complexes listed in Table V. But there are also distinct differences within the group of vanadium complexes with coordination spheres exclusively built up of sulfur functionalities.

Thus, in compound 1, a complex of tetrahedral geometry (if the persulfide is considered to occupy a single coordination site), the vanadium nucleus is less effectively deshielded than, e.g., in the tetrahedral thiovanadates $[\text{VS}_3\text{SH}]^{2-}$ and $[\text{V}_2\text{S}_6(\mu\text{-S})]^{4-}$ (cf. Table V). Apparently this is a consequence of the presence of persulfide; it has been previously demonstrated that replacement of an oxo by a peroxy group increases metal shielding.³² The

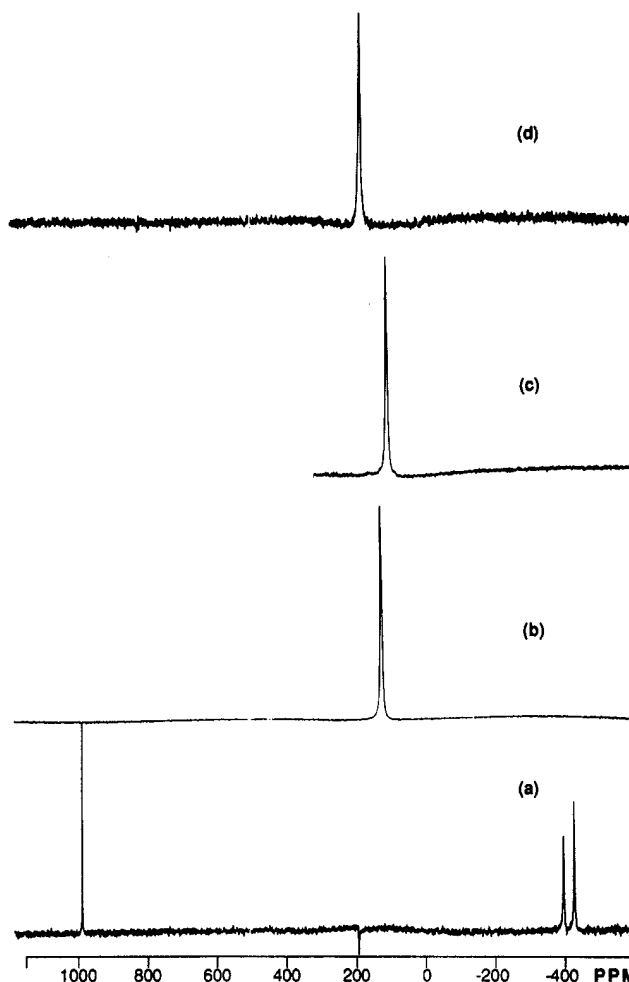


Figure 5. Stack plot of selected ^{51}V NMR spectra: (a) $[\text{V}(\text{S}_2)_2(\text{S}_2\text{SPh})]^{2-}$ (anion of 1); (b) $[\text{V}_2(\text{S}_2)_2(\text{CS}_3)_4]^{4-}$ (anion of 2); (c) $\text{V}_2(\text{S}_2)_2(\text{S}_2\text{CN}^n\text{Bu}_2)_4$ (4b); (d) $\text{V}_2(\text{S}_2)_2(\text{S}_2\text{CSMe})_4$ (3).

same is true for hydroxylamine (H_2NO^-) coordinating in the η^2 mode (cf. Table V). This effect has been rationalized in terms of the strain (nonoptimal overlap) present in a three-membered ring^{31,34} but may also, in the case of S_2^{2-} vs S^{2-} complexes, and in the light of the EHMO studies (vide supra), be traced back to a relatively large HOMO/LUMO gap for the $\text{V}_2(\text{S}_2)_2$ moiety.

Compounds 2–4 all have $\delta(^{51}\text{V})$ values between +103 and +173 ppm. With respect to 1, the ^{51}V nucleus is more effectively shielded by ca. 800 ppm. Again, this reflects the strain present in a chelate structure arising from replacement of the sulfide by the bidentate trithiocarbonato ligand, which gives rise to a rather small S–V–S angle of ca. 69° . An even higher shielding has been observed for $[\text{VO}(\text{OH})(\text{S}_2\text{CNEt}_2)_2]$,³¹ where, in addition to two four-membered rings, the O^{2-} and OH^- ligands induce an extra upfield shift. Within the group of thiocarbonato (ZCS_2^{2-}) complexes 2–4, the variation of $\delta(^{51}\text{V})$ is relatively small, indicating that, in solution, the thiocarbonato appears to coordinate in a bidentate fashion in all cases, and the electronic second-sphere influences from the group Z are small.

Acknowledgment. This work was supported by the Office of Basic Energy Sciences, Division of Chemical Sciences, U.S. Department of Energy, under Grant DE-FG02-87ER13702. We thank Mr. Joe R. Rambo (Indiana University) and Professor Odile Eisenstein (Laboratoire de Chimie Theorique, Centre de Paris-Sud, Orsay, France) for invaluable help with the extended Hückel calculations.

Supplementary Material Available: Textural and tabular summaries of the structure determinations, tables of atomic coordinates, thermal parameters, and bond distances and angles, and additional structural diagrams for complexes 1 and 2 (31 pages). Ordering information is given on any current masthead page.

(32) Harrison, A. T.; Howarth, O. W. *J. Chem. Soc., Dalton Trans.* **1985**, 1173.

(33) Rehder, D.; Wiegardt, K. Z. *Naturforsch., B* **1981**, *36*, 1251.

(34) Rehder, D. In *Transition Metal Nuclear Magnetic Resonance*; Pregosin, P. S., Ed.; Elsevier: Amsterdam, 1991; p 1.

(35) Mason, J., Ed. *Multinuclear NMR*; Plenum Press: New York, 1987.